Upper Ocean Circulation in the Northern South China Sea

Huijie Xue, Fei Chai, Neal Pettigrew
School of Marine Sciences, University of Maine, Orono, ME 04469-5741, USA

Danya Xu
South China Sea Institute of Oceanography, Guangzhou, China

Maochong Shi
Ocean University of Qingdao, Qingdao, China

Corresponding author: Huijie Xue (Phone: 207-581-4318; Fax: 207-581-4388; Email: hxue@maine.edu)

Abstract

The Princeton Ocean Model is used to study the circulation in the South China Sea (SCS) and its seasonal transition in response to alternating monsoon winds, Kuroshio intrusion and river runoffs. The model has an orthogonal curvilinear grid in the horizontal with a minimum grid spacing of 10 km in the northern shelf of the SCS, and 22 levels in the vertical. The model domain includes the Sulu Sea and a small area of the western Pacific Ocean east of Philippines. The North Equatorial Current, Kuroshio and Mindanao Current, as well as the inflows and outflows through the Taiwan Strait, Sulu Archipelagos and the Karimata Strait, are prescribed as the open boundary forcing.

This paper presents the results from a 20-year model integration. Time series of the transport across the Bashi Channel and the Taiwan Strait suggest that the upper ocean has reached an equilibrium state. Net transport through the Bashi Channel is inward for most part of the year and reaches maximum in the fall. Strong coastal currents are found on the northern shelf and off the coast of Vietnum. The coastal current is counter-clockwise in winter, and turns clockwise in summer. Upwelling occurs off the coast of Guangdong, Hainan, and Vietnam in summer. The direction of the river plume is controlled by winds. In winter the Pearl River diluted water moves westward and reaches as far as Hainan, whereas in summer, it moves eastward and reaches Taiwan Bank. The Kuroshio enters the SCS through the Bashi Channel often in the form of a loop current except that in the fall the Kuroshio water can move across the SCS as a part of the northern SCS slope current.

1. Introduction

The South China Sea (SCS) is a large tropical marginal sea that extends from the equator to 23°N and from 99°E to 120°E (Fig. 1). It plays a significant role in the formation of Southeast Asian Monsoon that affects all the bordering countries (Lau and Lau, 1992). The SCS is connected to the East China Sea, the Java Sea, and the Indian Ocean via a labyrinth of narrow and shallow sea straits. In contrast, its connection to the western Pacific through the Bashi Channel is deep and wide. Even though the deepest part of the SCS exceeds 5000 m, the exchange below the 200 m isobath occurs mostly in the Bashi Channel which gives rise to its semi-enclosed nature. Continental shelves are wide in the northern and southern SCS, but extremely narrow in the east and west.

The SCS is subjected to the strong forcing of alternating northeast and southwest monsoon winds, frequent typhoons, seasonal incursions of the Kuroshio Current, and fresh water inflows from the Pearl River and the Mekong River. Its large size, low latitude, and semi-enclosed nature add additional dynamical complexity that foretells of convergent shelf and coastal currents that may in turn engender counter currents, undercurrents and gyres in the shelf/slope region.

Due to the lack of direct current measurements, many of the prevailing notions about the currents in the SCS are derived from a combination of hydrographic distributions and modeling results (e.g., Zeng et al., 1989, Liu and Su, 1992, Mao et al., 1992, Li et al., 1994, Shaw and Chao, 1994, Cai and Su, 1995, Fang et al., 1998, Chu and Edmons, 1999). While these studies have stimulated a great deal of interest and raised important questions, the models have generally not been of sufficient resolution to adequately treat the complex mesoscale circulation field in the region.

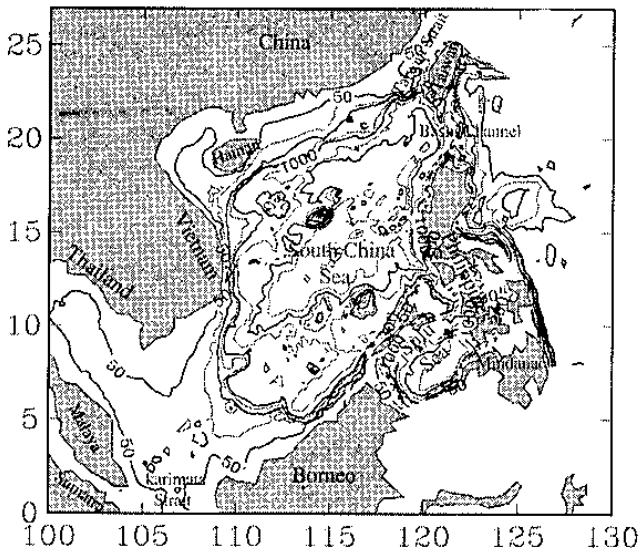

Fig. 1. Topography of the South China Sea. Contours are 50, 100, 200, 600, 1000, 2000, 3000, 4000, and 5000m, respectively.

In this study, the model domain is extended to include a small area of the western Pacific Ocean and the Sulu Sea, hence less constraints are imposed on the exchange between

the SCS and the neighboring regions, especially the excursion/incursion of the Kuroshio through the Bashi Channel. In addition, the present model has finer resolution in the northern SCS, adequate to resolve mesoscale eddies and other prominent circulation features there.

2. Model Setup

The three-dimension Princeton Ocean Model (Blumberg and Mellor, 1987) is configured for the SCS in an orthogonal curvilinear coordinate with a total of 151x101 grid points (Fig. 2). It has variable grid sizes. The densest coverage is in the northern shelf of the SCS where grid size ranges from 9 km at the coast to about 12 km at the shelf break. Resolution is also relatively high off the coasts of Vietnam and Philippines. The model has 22 sigma levels in the vertical with higher resolution in both the surface and the bottom boundary layer. The ETOPO5 data set is used to specify the bottom topography (Fig. 1). The maximum depth is set to 6000 m in the model.

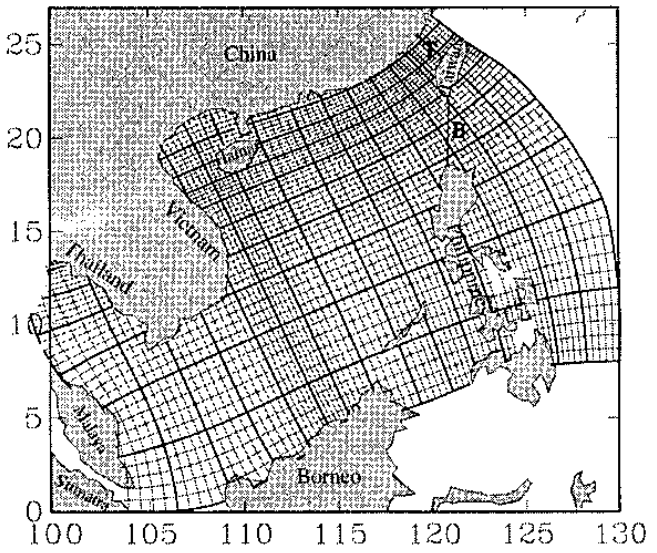

Fig. 2. Horizontal mesh of the South China Sea model at the half resolution. Transports through the Taiwan Strait (section T) and the Bashi Channel (section B) are shown in Figure 3.

At the surface, the model is forced with monthly climatological winds and net heat and fresh water fluxes from the Comprehensive Ocean Atmosphere Data Set (COADS). The SCS is under the strong and sometimes simultaneous influence of both the Southeast Asian and Indian Monsoon systems. Climatological data suggest that the winter northeast monsoon ends in April, and that winds in the region are generally weak during this time of year. The southwest monsoon first appears in the central basin in May and expands over the entire basin in July and August. The transition from summer to winter is characterized by the gradual southward advancement of northeast monsoon conditions. The northeast monsoon first appears over the northern shelf in September, at which time the southwest monsoon still prevail to the south. This convergent wind pattern, due to the great size of the SCS, will strongly influence the circulation on the shelf and over the slope. The northeast monsoon subsequently expands southward against the diminishing southwest monsoon during October, reaching its maximum in December and covering the entire SCS.

In addition to their strong winds, monsoons also bring excessive precipitation to the region with an annual averaged rainfall of 2 m. The resultant freshwater runoff into the SCS, especially from the Pearl River in the north and the Mekong River in the southwest, is large even by global standards. It plays an important role in the hydrographic and flow regimes on the shelf. Perry et al. (1996) estimated the annual averaged discharge rate at 15,000 m^3/s and 10,000 m^3/s for the Mekong River and the Pearl River, respectively. In the model, discharge from both rivers varies monthly according to the percentages given in table 1.

Table 1. Ratio of the monthly river discharge to the annual discharge.

Month	1	2	3	4	5	6
%	2.16	2.42	3.37	7.70	14.63	19.23
Month	7	8	9	10	11	12
%	13.92	13.25	10.37	6.00	4.06	2.90

There are two open boundaries in the model. To the east, the model is connected with the East China Sea (Taiwan Strait) and the western Pacific Ocean. To the south, the model is connected with the Java Sea (Karimata), the Celebes Sea (channels through Sulu Archipelagos), and the Pacific Ocean. The model open boundary condition is obtained from the Navy Postgraduate School 1/4° x 1/4 ° Parallel Ocean Climate Model (POCM) 10 year climatology between 1988 and 1997.

The model is initialized with the POCM 10 year January average. It is then integrated forward in time with monthly forcing for 20 years. Model results are saved every 5 days. Figure 3 shows the transport through the Taiwan Strait and the Bashi Channel and the kinetic energy in the upper 800 m throughout the 20-year model integration. It appears that shallow areas have reached equilibrium such that the transport through the Taiwan Strait has attained a steady annual cycle (Fig. 3a). There is a low frequency modulation in the transport through the Bashi Channel since a large portion of the channel is deeper than 1000 m, suggesting a longer integration period is needed for the deep SCS to reach equilibrium. Although the upper ocean kinetic energy is still highly variable and without apparent annual cycle (Fig. 3b), the 1-year lowpass filtered time series shows the kinetic energy in the upper 800 m oscillates around a relatively steady level during the second half of the integration period.

3. Results

Monthly averages of temperature, salinity, velocity and elevation have been calculated from the archived model results to illustrate the seasonal transition of the circulation pattern in the SCS. This paper focuses on the northern SCS, and only a portion of the model domain (from 12°N to 27°N, from 100°E to 122.5°E) is shown in subsequent figures for clarity. Coastal currents on the northern shelf, the South China Sea Warm Current, Kuroshio incursion and the slope current, and the anticyclone west of the Bashi Channel are discussed in the following sections.

3.1 Coastal currents

Figure 4 shows the vertically averaged velocity, in which currents in shallow regions stand out more clearly. Coastal

currents in the northern SCS have the most apparent seasonal alternation due to the strong monsoon forcing. The winter regime (Fig. 4a) lasts from November to February, whereas the summer regime (Fig. 4b) lasts from May to September. March and April are the winter-to-summer transition months, and October is the summer-to-winter transition month.

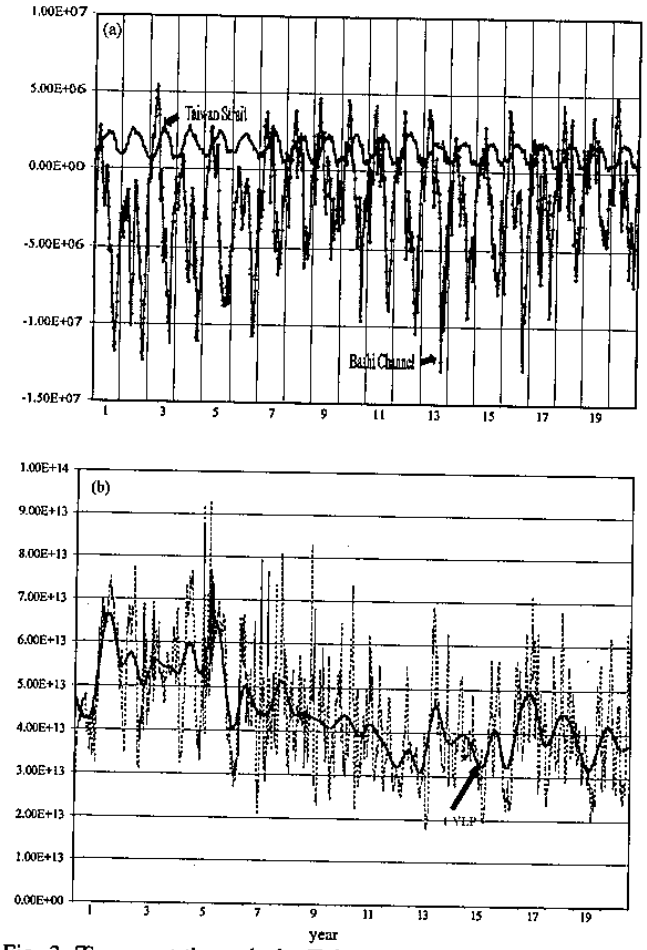

Fig. 3. Transport through the Taiwan Strait and Bashi Channel (a), and kinetic energy in the upper 800 m (b). The dashed curve in (b) is the time series calculated using the model output of every 5 days, and the solid curve is the 1 year lowpass filtered time series.

In winter, the strong northeasterly monsoon causes the water to accumulate on the western side of the SCS. The combination of the wind-driven and gradient forcing result in a westward and southward coastal current system off the coasts of China and Vietnam. The Guangdong Coastal Current flows from northeast toward southwest. It is stronger east of the Pearl River estuary (about 20 cm/s) compared to about 15 cm/s west of the estuary. The coastal current splits northeast of Hainan, part of it moving through the Qiongzhou Strait and becoming a counter-clockwise flow in the Gulf of Tonking and part of it turning southward and becoming the Hainan Coastal Current. The latter is joined by a westward flow north of Xisha. It is about 200 km wide with speeds of 10-25 cm/s at the mouth of the Gulf of Tonking. The Vietnam Coastal Current is even stronger after it converges with the westward flows from the interior basin of the SCS.

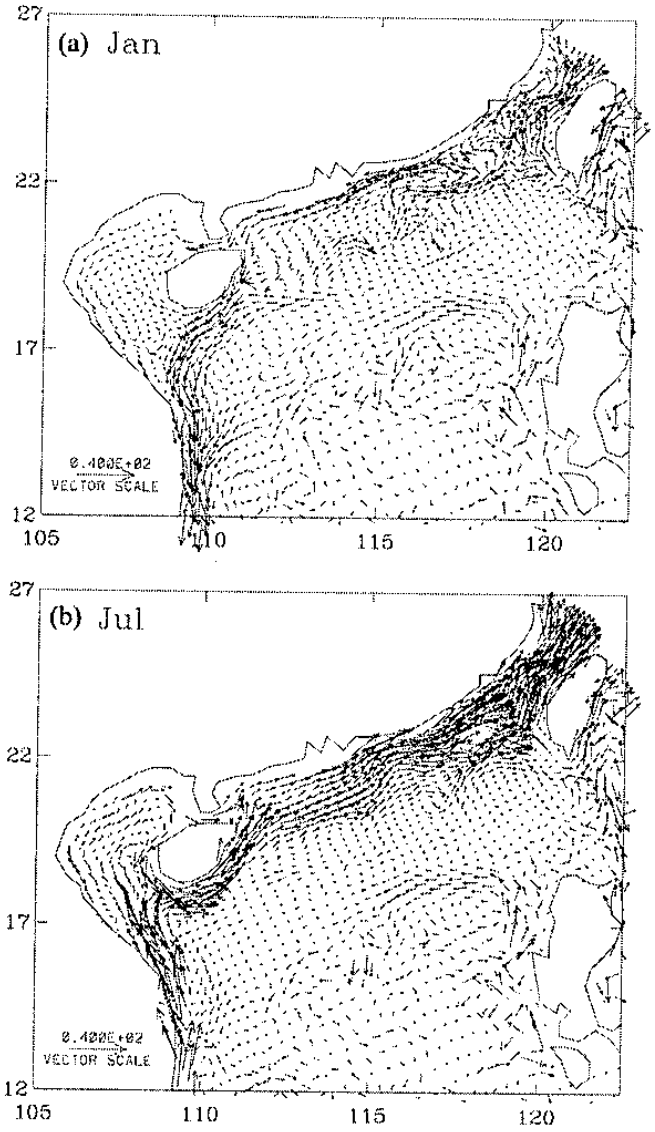

Fig. 4. Vertically averaged velocity in January (a) and July (b).

In summer, the southwest monsoon drives the water away from the western and northern coasts of the SCS, and the coastal currents reverse their directions. The Vietnam Coastal Current is northward with speeds of 30-40 cm/s. A large excursion appears at the mouth of the Gulf of Tonking. The current on the northern shelf is broad, and it is strengthened east of the Pearl River estuary because of the Pearl River outflow.

Effect of the Pearl River outflow is to the west of the Pearl River estuary in winter (Fig. 5a). Low salinity water enters the Gulf of Tonking through the Qiongzhou Strait. As a result, salinity is lower than 33 psu in the northern Gulf of Tonking. In summer, the majority of the river outflow turns to the east. The Pearl River diluted water moves past the Taiwan Strait, and could affect water properties in the East China Sea. Salinity is about 29 at 115°E and 32 near Taiwan Bank. Westward expansion of the river plume is limited by the southwest monsoon in summer.

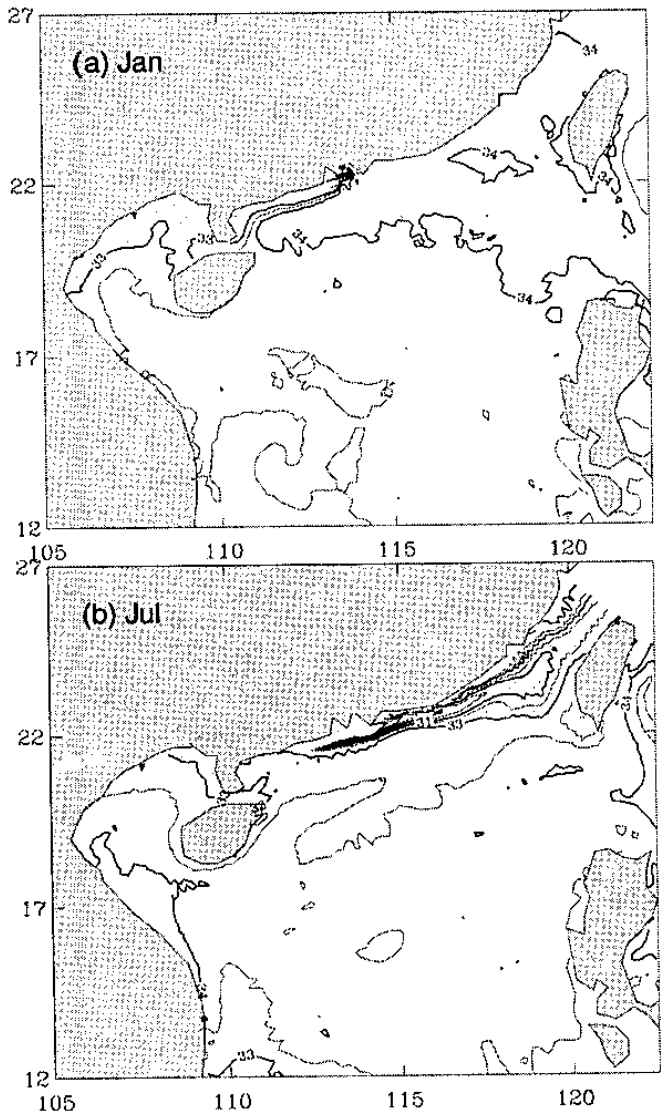

Fig.5 Surface salinity in January (a) and July (b). Contour interval is 1 for salinity ≤ 33, but 0.5 for salinity > 33.

3.2 Coastal upwelling

During summer, southwest monsoon drives offshore water movement and generates upwelling along the western and northern coasts of the SCS. Figure 6 shows the surface temperature in July. There are two obvious cold regions. One extends from Hong Kong to the northern end of the Taiwan Strait, another expands the coast of Vietnam from 10°N to 19°N. The minimum temperature of both upwelling zones is 25-26°C, about 3-4°C cooler than the water 100 km offshore. A smaller and weaker upwelling zone is located east of Hainan where the mimimum temperature is about 28°C. These three upwelling regions were observed by Guan and Chen (1964), Han and Ma (1988), Han et al (1990), Yan (1992), and Deng et al (1995). Model results compare favorably with observations for the regions off the coasts of eastern Guangdong and Vietnam. However, the upwelling east of Hainan appears too weak in the model.

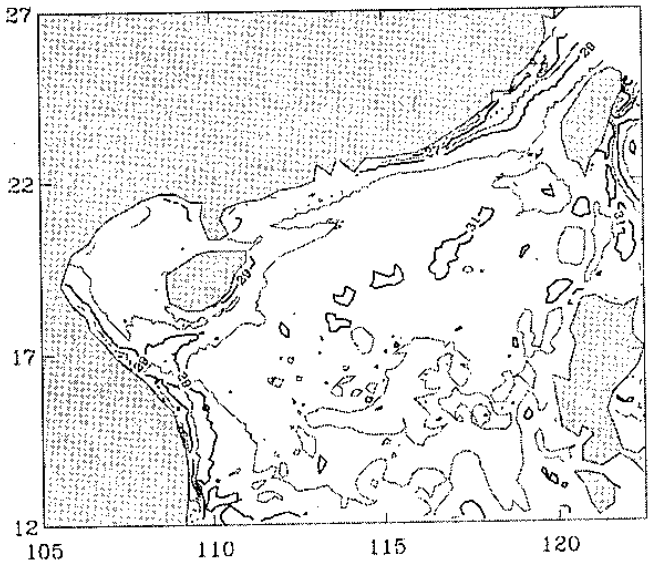

Fig.6. Sea surface temperature in July. Contour interval is 1 °C.

3.3 The South China Sea Warm Current (SCSWC)

The SCSWC, an eastward flowing current along the continental shelf break from 115°E to 120°E, is well simulated in the model (Fig. 4a). It is about 100 km wide with a sustained vertically averaged velocity of 15 cm/s, in good agreement with the observations obtained by Guan (1978a, 1978b, and 1985), Guo et al (1985), Ma et al. (1990), and Huang and Zheng (1996).

Although not shown, the SCSWC appears to be weak and unorganized at the surface. It is still unorganized at 20m depth in November and December, but much better defined in January and February. At 50 m (Fig. 7a), the SCSWC is sustained from November to February the following year and is quite similar to its vertical average seen in Fig. 4a, near the shelf break with a width of 100 km, length of 500 km, and maximum velocity of 20 cm/s. Temperature of the SCSWC is about 1-2°C warmer than the surrounding water. The SCSWC at 200 m is similar to that at 50 m except that the current becomes a little narrower.

The main water source of the SCSWC is a mixture of the slope water and the Kuroshio water. The Kuroshio water moves west- and northwestward after entering the Bashi Channel. It mixes with the slope water and splits near Dongsha with one part continuing westward as the slope current and the rest turning eastward and becoming the SCSWC. The most striking features of the SCSWC are that it is against the prevailing wind and that it flows along the shelf break. Both the barotropic and the baroclinic gradient are important in the formation of the SCSWC. Waters move northward on the slope that results in convergence hence a high elevation zone parallel to the shelf break. Geostrophic flow is thus eastward (against the wind direction) on the northern side of the high elevation zone as suggested by Yuan and Deng (1997 and 1998). Furthermore, the convergence due to the northward moving water on the slope not only generates a zone of elevated sea level, but also sinking motions on the offshore side of the shelf break. Since the mixture of the

Kuroshio water and the slope water is relatively warm, there forms a warm band on the slope. A warm zone is also a zone of high dynamic height. Therefore, the current on the offshore side of the shelf break is again eastward.

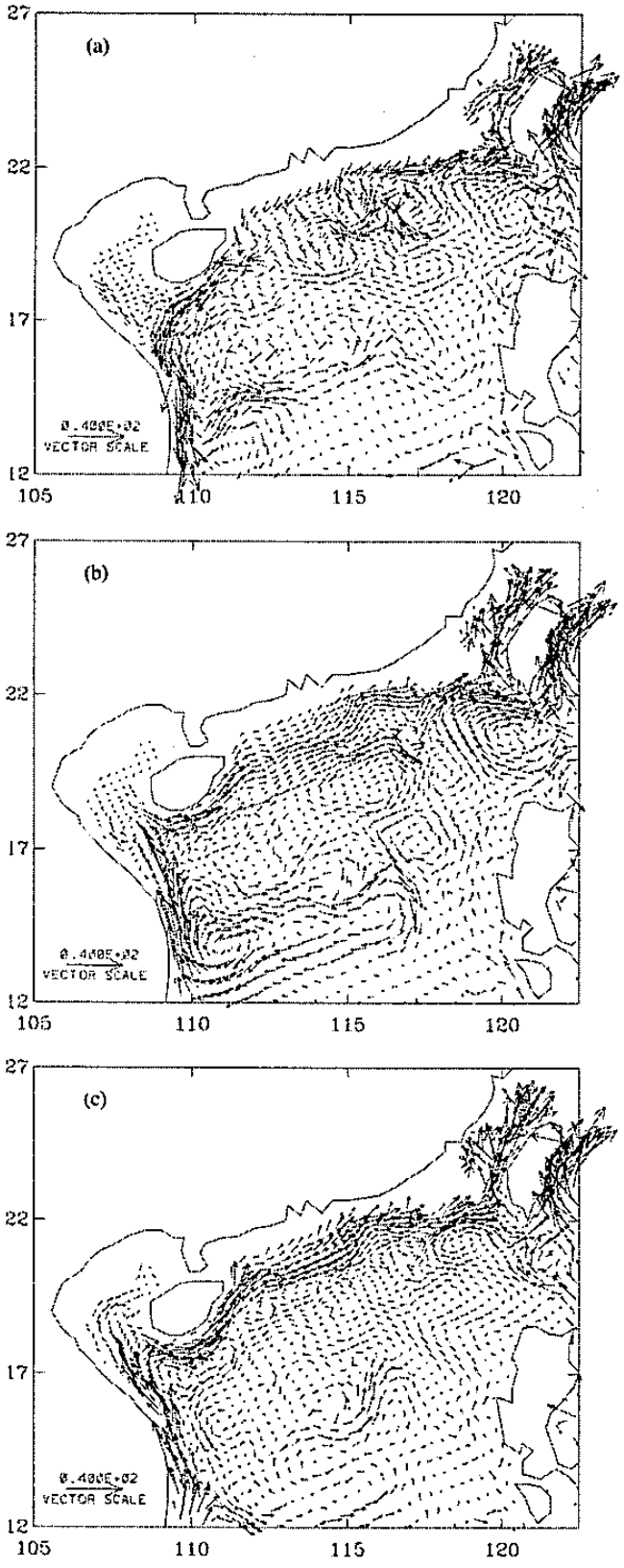

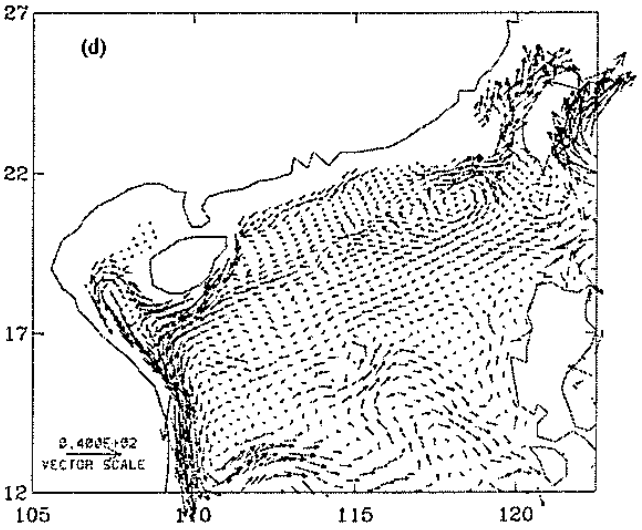

Fig. 7. Velocity at 50 m in January (a), April (b), July (c), and October (d).

3.4 Kuroshio excursion/incursion

Kuroshio excursion and the westward movement of the Kuroshio water on the northern slope of the SCS were observed by Qiu et al (1984), Guo et al (1985), Li and Wu (1989) and Xu and Su (1997). Fig.3a shows that the net transport through the Bashi Channel is inward from June to January the following year but outward from February to April. The net inflow is the largest in the fall and it is expected that the influence of the Kuroshio on the SCS is the greatest at that time of year.

At 50m, the inflow of the Kuroshio takes the form of a loop current in January and April (Fig. 7a and 7b), entering on the south side of the Bashi Channel and exiting on the north side. The western edge of the loop is at about 118°E. Furthermore, the loop current encompasses an anticyclonic eddy with its center located at about 120°E. In July, the loop current extends farther west, reaching the south of Dongsha (Fig. 7c). By October, the Kuroshio water moves across the northern slope of the SCS and becomes a part of the northern SCS slope current. The anticyclonic eddy shifts farther to the west and its center is now located at 118°E (Fig. 7d). During most time of the year, the northern branch of the loop current separates southwest of Taiwan, and part of it turns northward to become the Taiwan Warm Current.

4. Summary

The Princeton Ocean Model has been configured for the SCS with unprecedentedly high resolution in the northern shelf/slope region of the SCS. The model has been integrated forward in time for 20 years with climatological monthly forcing, and the upper ocean has attained a quasi-equilibrium annual cycle. The model shows the seasonally alternating coastal currents, the SCSWC in the winter, and the summertime eastern Guangdong coastal upwelling that are in good agreement with observations. The Pearl River outflow turns westward in the winter and the low salinity water passes the Qiongzhou Strait and affects the Gulf of Tonking. In summer, however, most of the Pearl River outflow turns eastward and its influence reaches the Taiwan Strait and

beyond whereas the westward expansion is limited by the prevailing southwesterly winds. The Kuroshio enters the SCS through the Bashi Channel in the form of a loop current during most time of the year. As the season progresses, the loop current extends farther to the west. By fall, the Kuroshio water moves across the SCS as a part of the northern SCS slope current.

The archived model results are also being used to calculate convergence, vorticity, and energy in aid of our understanding the dynamics of the SCSWC, the Kuroshio incursion, mesoscale eddies, and the SCS circulation in general. Furthermore, the model is continuously being integrated forward in time, with which we hope to learn about the adjustment processes in the deep SCS.

5. References

Blumberg, A. F., and G. L. Mellor. 1987:A Discription of a Three-Dimensional Coastal Ocean Circulation Model. Three-Dimensional Coastal Ocean Models, N.Heaps ed., Amer. Geophys. Union, 4, 1-16.

Cai, S.-Q., and J.-L. Su. 1995: Two Layer Model of the Circulation in South China Sea. Acta Oceanologica Sinica, 17(2), 12-19.

Chu, P.C., and N.L. Edmons, 1999: A Three-Dimensional Numerical Simulation of the South China Sea Circulation and Thermohaline Structure. Chinese J. of the Atmos. Sci., 22, 481-503.

Deng, S., H.-L. Zhong, M.-W. Wang, F.-J. Yun. 1995: On Relation Between Upwelling off Qionghai And Fishery . J. of Oceanog. in Taiwan Strait, 14, 51-56.

Fang,, G.-H., W.-D. Fang,, Y. Fang, and K. Wang. 1998: A Survey of Studies on the South China Sea Upper Ocean Circulation. Acta Oceanograpjica Taiwania, 37, 1-16.

Guan, B.-X. 1978a: The Worm current in the South China Sea: A Current Against the Wind in Winter in the Open Sea off Guang Dong Province. Oceanologia Et Limologia Sinica, 9, 117-127.

____. 1978b: The New Evidence of the warm current of South China Sea. Marine Sciences Supplement, 100-103.

____. 1985: Some Feature of the Temporal and Spatial Distribution of the "Counter-Wind" in Northern South China Sea in Winter. Oceanologia Et Limologia Sinica, 16, 429-437.

____, and X.-J. Chen. 1964: The Current Regime of the China Adjacent Seas. In Report of the National Ocean Comprehensive Survey, 5(6), 1-85.

Guo, Z.-X., T.-H. Yang , and D.-Z. Qiu. 1985: South China Sea Warm Current and a Southwestward Current on its Right Side in Winter. Tropic Oceanology, 4, 1-9.

Han, W.-Y., and K.-M. Ma. 1988: The Study of Upwelling Along the East Coast of Guang Dong Province. Acta Oceanologica Sinica, 10, 52-59.

____, M.-B. Wang, and K.-M. Ma. 1990: On the Lowest Surface Water Temperature Area of China Sea in Summer—the Upwelling Along the East Coast Of Hai Nan Island. Oceanologia Et Limologia Sinica, 21, 261-275.

Huang, Q.-Z., and Y.-R. Zheng. 1996: The currents in Northeastern Paart of South China Sea and Ba shi Strait in March, 1992. Oceanography in China, 6, 42-52.

Lau, N.-C., and K.-H. Lau. 1992: Simulation of the Asian Summer Monsoon in a 40-year Experiment with a General Circulation Model. East Asia and Western Pacific Meteorology and Climate. W.J. Kyle and C. P. Chang Eds., World Scientific Publishing Co., 49-56.

Li, L., and B.-Y. Wu. 1989: The Current Lasso of Kuroshio in South China Sea: The Study of Circulation Structure in Northeastern Part of South China Sea. J. of Oceanog. in Taiwan Strait, 8, 89-95.

Li, R.-F., Q.-Z. Huang, and W.-Z. Wang. 1994: Numerical Simulation of the Upper Layer Current in South China Sea. Acta Oceanologica Sinica,16, 13-22.

Liu, X.-B., and J.-L. Su. 1992: Reduced Gravity Model of the Circulation in the South China Sea. Oceanologia Et Limologia Sinica, 23(4), 167-174.

Ma, Y.-L. 1990: The Report of Decadal Hydrographic Series Survey of the Shelf and Adjacent Waters of the Northern South China Sea. China Ocean Press, Bei Jing, 254 pp.

Mao, M, W.-Z. Wang, and Q.-Z. Huang. 1992: Three Dimension Numerical Experiment of Circulation in South China Sea. Tropic Oceanology, 11(4), 34-41.

Perry, G. D., P. B. Duffy, and N. L. Miller, 1996: An extended data set of river discharges for validation of general circulation models. *J. Geophys. Res.*, 101, 21339-21349.

Qiu, D.-Z., T.-H. Yang, and Z.-X. Guo. 1984: A westward Current in the Northeastern Part of South China Sea in Summer. Tropic Oceanology, 3, 65-72.

Shaw, P.-T., and S.-Y. Chao. 1994: Surface Circulation in the South China Sea. Deep Sea Res., 41, 1663-1683.

Xu, J.-P., and J.-L. Su. 1997: The Hydrological Analysis About Kurushio Invading South China Sea: Observational Results in Aug.-Sep., 1994. Tropic Oceanology, 16, 1-23.

Yan, T.-Z. 1992: The Analysis About Cause of Formation of Upwelling Along the Coast of Zhe Jiang Province and the East Coast of Hai Nan Island. Acta Oceanologica Sinica, 14, 12-18.

Yuan, S.-Y., and J.-Z. Deng. 1997: A Primary Study of Winter and Summer Upwind Flow Mechanism in the Northern Part of South China Sea. Tropic Oceanology, 16, 63-69.

____, and ____. 1998: A Numerical Experiment of Winter Upwind Flow in the Northeastern Part of South China Sea. Tropic Oceanology, 17, 26-31.

Zeng, Q.-C., Li R.-F., Z.-Z. Ji, Z.-J. Gan, and P.-H. Ke. 1989: Calculation of Monthly mean Currents of the South China Sea. Chinese J.of Atmospheric Sciences, 13, 127-138.